β-Very Low Density Lipoprotein Is Sequestered in Surface-connected Tubules in Mouse Peritoneal Macrophages

Jeffrey N. Myers,* Ira Tabas,‡ Nancy L. Jones,§ and Frederick R. Maxfield*

*Departments of Pathology and Physiology, ‡Medicine, and Anatomy and Cell Biology, Columbia University College of Physicians and Surgeons, New York 10032; and §Department of Pathology, Bowman Gray School of Medicine of Wake Forest University, Winston-Salem, North Carolina 27157

Abstract. β-very low density lipoprotein (VLDL) is a large lipoprotein with multiple apoprotein E (apoE) molecules that bind to the LDL receptors on mouse macrophages. Even though they bind to the same receptor, the endocytic processing of β-VLDL differs from low density lipoprotein (LDL). LDL is rapidly delivered to perinuclear lysosomes and degraded, but much of the β-VLDL is retained in peripheral compartments for several minutes. We have investigated the properties of these peripheral compartments. Measurement of the pH was made using FITC-phosphatidylethanolamine incorporated into the β-VLDL, and we found that the peripheral compartments were near neutral in pH. These peripheral, β-VLDL containing compartments were poorly accessible to antibodies, but a low molecular weight fluorescence quencher (trypan blue) entered the compartments within a few seconds. Intermediate voltage EM of cells labeled with colloidal-gold-β-VLDL revealed that the peripheral compartments are tubular, surface-connected invaginations. Kinetic studies with fluorescent β-VLDL showed that the compartments become fully sealed with a half-time of 6 min, and the β-VLDL is then delivered rapidly to perinuclear lysosomes. By monitoring fluorescence energy transfer between lipid analogs incorporated into the β-VLDL, some processing of the lipoprotein in the peripheral tubular compartments is demonstrated. The novel mode of uptake of β-VLDL may account for the high cholesterol ester accumulation induced by this lipoprotein.

MACROPHAGES and other phagocytic cells possess mechanisms for the internalization of a wide variety of extracellular ligands. In addition to receptor-mediated endocytosis, macrophages can internalize large, multivalent ligands by phagocytosis (Griffin et al., 1975) and large volumes of fluid by macropinocytosis (Swanson, 1989). Recent research by several groups has begun to uncover the extensive interrelations among these processes (Mayorga et al., 1991; Rabinowitz et al., 1992), but the detailed intracellular itineraries followed by multivalent ligand–receptor complexes remain poorly understood. The low density lipoprotein (LDL)[1] and β-very low density lipoprotein (VLDL) β-VLDL provide a physiological model system in which monovalent and multivalent ligands exist for the same receptor. The apo-B,E receptor, or macrophage LDL receptor, binds both LDL, which contains a single copy of apoB, and β-VLDL, a large lipoprotein that contains one apoB and multiple apoE molecules (Fainaru et al., 1982). Research from our laboratories has shown that despite binding to the same receptor, LDL and β-VLDL follow divergent endocytic pathways in mouse peritoneal macrophages. LDL is rapidly delivered to perinuclear lysosomal compartments, but a significant fraction of β-VLDL remains in the cell periphery for several minutes (Tabas et al., 1990). By EM, β-VLDL appears to be in electron-lucent vesicles while LDL is rapidly delivered to electron-dense compartments that have the characteristics of lysosomes. In addition, β-VLDL is degraded more slowly than LDL, although both lipoproteins are rapidly internalized, as assessed by suramin releasability. More recently we have demonstrated that the peripheral distribution of β-VLDL is due to the multivalency of apoE on the lipoprotein particle, and not its large size alone (Tabas et al., 1991). In all of our experiments thus far, the existence of peripheral compartments containing β-VLDL has correlated with increased activity of the enzyme acyl-CoA/cholesterol acyl transferase (ACAT), which esterifies

Address all correspondence to F. R. Maxfield, Ph.D., Department of Pathology, Columbia University, 630 West 168th Street, New York, NY 10032.

1. *Abbreviations used in this paper*: α_2M, α_2 macroglobulin; ACAT, acyl-CoA/cholesterol acyl transferase; AFA, anti-fluorescein antibody; apoE, apoprotein E; CCD, charge-coupled device; DHB, DME with Hepes and BSA; DiI, 1,1′-dioctadecyl-3,3,3′,3′-tetramethylindocarbocyanine perchlorate; DiO, 3,3′- dioctadecyloxacarbacananine perchlorate; FPE, fluorescein phosphatidylethanolamine; FRET, fluorescence resonance energy transfer; IVEM, intermediate voltage electron microscopy; LDL, low density lipoprotein; LPDS, lipoprotein-deficient serum; TR, Texas red; VLDL, very low density lipoprotein.

cellular free cholesterol (Brown and Goldstein, 1983). ACAT activation is believed to be the key regulated step necessary for the accumulation of cholesteryl esters in macrophages (Tabas et al., 1986) that leads to the formation of the "foam cells," which are prominent in atherosclerotic lesions in vivo (Fagiotto et al., 1984; Gerrity, 1981; Schaffner et al., 1980). Thus, it is possible that a mechanistic link exists between the peripheral β-VLDL compartments and ACAT activation.

The goal of the present study was to characterize the peripheral compartments containing β-VLDL. We found that β-VLDL is removed from the cell surface into a compartment that is accessible to small molecules in the external milieu. This compartment remains at a neutral pH and lacks lysosomal markers, but some processing of the β-VLDL occurs nonetheless. By EM, the peripheral β-VLDL appears to reside in long (>1 μm) tubular compartments ~250 nm in diameter. Eventually, the β-VLDL containing compartment closes from the plasma membrane, becomes acidic, and is rapidly transported to the perinuclear region of the cell where it acquires lysosomal markers. These results suggest that the widely distributed β-VLDL compartment represents a pre-endocytic state in which the β-VLDL is sequestered from the cell surface but not completely internalized.

Materials and Methods

Cells

Peritoneal macrophages from unstimulated female ICR mice (15–25 g; Harlan Sprague Dawley, Inc., Indianapolis, IN) were plated onto poly-D-lysine–coated coverslip-bottom dishes and incubated for 2 d in DME/10% (vol/vol) lipoprotein-deficient serum (LPDS) as previously described (Tabas et al., 1990). All experiments were performed on day 3. CHO fibroblasts (cell line TRVbl) were cultured as described in Dunn and Maxfield (1992).

Lipoproteins and Proteins

Human LDL was prepared as previously described (Tabas et al., 1990). β-VLDL from cholesterol-fed rabbits was prepared by ultracentrifugation at a density of 1.006 gm/ml (Innerarity et al., 1982). The $d < 1.006$ lipoproteins, which contain mostly β-VLDL but also some pre-β-VLDL, will be referred to as simply "β-VLDL." β-VLDL was labeled with 1,1'-dioctadecyl-3,3,3',3'-tetramethylindocarbocyanine perchlorate (DiI) or both DiI and 3,3'-dioctadecyloxacarbacanine perchlorate (DiO) (all fluorescent probes from Molecular Probes, Eugene, OR) by the method of Pitas et al. (1981) and stored at 4°C under argon, with 50 U/mL penicillin G, 50 μg/ml streptomycin (GIBCO BRL, Gaithersburg, MD). When β-VLDL was labeled for energy transfer experiments, lipoprotein samples were labeled with several different mixtures of DiO and DiI. We had shown in our previous work that DiI or DiO labeling of β-VLDL did not perturb the biochemical properties of β-VLDL in macrophages, and were appropriate probes of β-VLDL endocytosis (Tabas et al., 1990). Labeling of β-VLDL with fluorescein phosphatidylethanolamine (FPE) was carried out using an identical protocol to that for DiI, except that only 50 μg FPE was added per mg β-VLDL protein, rather than 150 μg as with DiI. Over-labeling of β-VLDL with FPE resulted in nonspecific binding to the cells; therefore, every preparation of FPE–β-VLDL (as well as DiI–β-VLDL) was tested for specificity of binding by competition with excess unlabeled β-VLDL. β-VLDL was labeled with ^{125}I (IMS.30; carrier-free; Amersham Corp., Arlington Heights, IL) using iodine monochloride as described in detail previously (Goldstein et al., 1983). DiI–β-VLDL was labeled with 26-nm colloidal gold as described previously (Jones et al., 1991) and dialyzed into DHB (DME, 10 mM Hepes, 0.2% fatty acid-free BSA, pH 7.4). Gold DiI–β-VLDL was tested for specificity by competition with unlabeled β-VLDL; nonspecific binding was negligible. β-VLDL, LDL and other proteins were analyzed for protein content by the method of Lowry et al. (1951). Human α_2-macroglobulin (α_2M) was purified, converted to the receptor-binding form, and conjugated to fluorescein isothiocyanate or Texas red as previously described (Salzmann and Maxfield, 1989).

Antibodies and Immunofluorescence

Polyclonal antibody against apoE (GBE-2, sheep antiserum) was kindly provided by Dr. Karl Weisgraber (Gladstone Foundation Laboratories, University of California, San Francisco, CA). For immunofluorescence experiments 5% (vol/vol) normal sheep serum (Calbiochem Corp., La Jolla, CA) was used as a control; nonspecific binding of GBE-2 under these conditions was negligible. In the absence of β-VLDL, a small amount of endogenous apoE could be visualized using the anti-apoE, but the intensity of the labeling was insignificant compared with the amount of antibody bound in the presence of β-VLDL. mAb against LAMP-1 (1D4B, rat IgG_{2a}) was kindly provided by Dr. Thomas August (The Johns Hopkins University, Baltimore, MD) (Hughes and August, 1989). Normal rat serum (Calbiochem, Corp.) was used for the nonspecific control with anti-LAMP-1; nonspecific binding was negligible. Rabbit anti-fluorescein antibody (AFA) was prepared and characterized in our laboratory as previously described (Salzmann and Maxfield, 1988).

For immunofluorescence experiments, cells were first fixed for 10 min at room temperature in PBS (0.13 M NaCl, 5 mM KCl, 20 mM sodium phosphate, pH 7.4) containing 4% (wt/vol) paraformaldehyde. In the anti-apoE experiments, cells were incubated in DME + 5% (vol/vol) sheep serum, either with or without the antibody GBE-2, for 30 min at room temperature. The samples were then rinsed and incubated for 45 min in PBS containing 2 mg/mL ovalbumin, and then incubated with fluorescence labeled second antibody in PBS–ovalbumin for 30 min at room temperature. After a final incubation with PBS–ovalbumin for 45 min, cells were viewed in the fluorescence microscope as described below. The same protocol was used for the anti–LAMP-1 experiments, except that normal rat serum was used for the nonspecific control, and cells were permeabilized by including 0.1 mg/mL saponin in antibody buffers.

Fluorescence Microscopy

Cells were incubated as indicated in the individual figure legends or text, rinsed, formaldehyde-fixed where indicated, and viewed by video intensification fluorescence microscopy using the Leitz Diavert microscope system and filter sets described previously (Tabas et al., 1990). Tape-recorded images were digitized with a Gould-Vicom IP 8400 image processor, and photographs were produced with a Polaroid Freeze Frame. Some images (as indicated) were recorded with a cooled charge-coupled device (CCD) camera (Photometrics CH250, Tucson, AZ) using a Kodak KAF1400 chip (Eastman Kodak Co., Rochester, NY). Adjacent pixels were binned by a factor of two in both the x and y dimensions, to yield a resolution of 660 (x) by 517 (y), and the images were digitized to a resolution of 12 bits. Photographs of CCD-recorded images were taken directly from the display of the image acquisition workstation.

pH Measurements

pH measurements were performed in a manner similar to that described in Maxfield (1989). After incubating the cells as described in the text, the cells were rinsed with room temperature (18–22°C) NSS (normal saline solution; PBS + 1 mM Mg^{2+} + 2 mM Ca^{2+}) and immediately placed on the microscope. After recording the Texas red (TR) α_2M image, pairs of images of FPE–β-VLDL compartments were recorded through a 530-nm bandpass emission filter, using sequentially 450 and then 490 nm illumination. Image pairs were recorded both before and after trypan blue addition. Finally, methylamine (20 mM) was added to neutralize the pH of acidic compartments and another 490-nm image was recorded. After digitization all images were background corrected and individual compartments isolated using routines described previously (Maxfield and Dunn, 1990). Both before and after trypan blue addition, the total 450 nm intensity for each compartment was divided by the corresponding total 490-nm intensity, and the pH of the compartment was evaluated by reference to a calibration curve of pH vs. 450/490 ratios. The calibration curve was prepared using FPE–β-VLDL in fixed cells equilibrated with buffers of known pH. The pH dependence of the fluorescence of FPE–β-VLDL in fixed cells (see Fig. 3, *inset*) was similar to that observed for other fluorescein-labeled proteins in living cells. This was consistent with previous studies in which fluorescent PE labels were incorporated into the outer, phospholipid monolayer of the β-VLDL and the fluorophore was exposed to the aqueous phase (Johnson et al., 1980).

Kinetics Experiments

The amount of FPE-β-VLDL that was exposed to the external milieu was evaluated using trypan blue quenching of fluorescein fluorescence. Trypan blue does not penetrate intact membranes and is widely used in cell sorting experiments to quench fluorescence signal from externally bound immune complexes containing fluorescein-labeled antibodies (Hed et al., 1987; Van Strijp et al., 1989; Weersink et al., 1990). Cells were incubated at 4°C for 30 min with FPE-β-VLDL at a concentration of 10 μg/ml. After rinsing with 37°C DHB, cells were chased at 37°C in DHB in the absence of ligand for the indicated times. After the 37°C chase, the cells were rinsed with room temp. (20–22°C) NSS, methylamine was added to 20 mM, and the cells were placed on the microscope, all within <60 s. A field of cells was selected using the phase-contrast optics, and a FPE-β-VLDL image was immediately recorded both before and after addition of trypan blue to a concentration of 2 mg/ml. Only 5–10 s elapsed between recording the images before and after trypan blue addition. The FPE-β-VLDL images were digitized and processed as described above to isolate individual compartments, and the ratio of the total intensity after trypan blue addition to before trypan blue addition was calculated for each compartment. Photobleaching and vesicle movement were negligible during the time scale (5–10 s) of the experiment.

Resonance Energy Transfer

Double-labeled β-VLDL was prepared as described above. Cells were incubated as indicated in the text and figure legend, rinsed with PBS, and fixed for 5 min at room temperature in 4% formaldehyde. Fluorescence microscopy was as described above, but a fluorescein and DiI optimized dual dichroic mirror was used for detection of DiO and DiI, respectively, with accessory excitation and emission optics (Omega Optical Inc., Brattleboro, VT). In intact particles the donor (DiO) fluorescence is strongly quenched and the particles appear red, from acceptor (DiI) fluorescence (Herman, 1989; Uster and Pagano, 1986). As the particle is disrupted, the quenching of donor is relieved, resulting in an increase in green fluorescence, and the particle color shifts in color from red to orange and then green, as the DiO fluorescence increases. Images were recorded using the cooled CCD camera system, and after background correction and isolation of individual compartments as described for pH analysis, the ratio of DiO to DiI fluorescence was calculated using the total intensities of the two labels in each compartment. The ratio values were scaled to fill the range of the display, and pseudocolored to represent the observed visual change in particle color from red to green as the β-VLDL is disrupted.

Electron Microscopy

For EM autoradiography, mouse peritoneal macrophages were cultured as described above, but were plated on 35-mm tissue culture plastic dishes (Becton-Dickinson, Oxnard, CA). On day 3, ^{125}I-β-VLDL was incubated with the cells for 6 min at 37°C, unbound ligand was washed away, and the cells were chased for 0 min or for 2 min at 37°C. The cells were processed for enhancement of membranes according to the method of Guyton and Klemp (1989): after fixation in glutaraldehyde, postfixation in osmium tetroxide, the samples were treated with 1% tannic acid, and then 1% paraphenylenediamine. The samples were then dehydrated in graded ethanol washes, embedded in Epox (Ernest F. Fullam, Inc., Latham, NY), and thin sections were cut parallel to the plane of the cell monolayer. Autoradiography was performed as described in Gershon and Sherman (1987), except that the samples were not stained with uranyl acetate and lead citrate. The sections were exposed for 4 wk, developed, and photographed at 12,000× using a JEOL 1200EX electron microscope (JEOL Ltd., Tokyo, Japan).

For thick-section intermediate-voltage EM (IVEM), samples were prepared in a manner similar to Jones et al. (1991). Cells were cultured as above, and on day 3 the cells were incubated with 26-nm gold-labeled DiI-β-VLDL for 5 min at 37°C, and chased with DHB in the absence of ligand for 5 min at 37°C. The cells were rinsed with 0.1 M sodium cacodylate buffer, pH 7.2, and fixed for 15 min at room temperature in cacodylate buffer containing 2.5% glutaraldehyde and 1% tannic acid (both from Electron Microscopy Sciences, Fort Washington, PA) to enhance membranes. However, the cells were not treated with para-phenylenediamine in these experiments. The samples were postfixed for 5 min in 0.1 M cacodylate buffer containing 1% osmium tetroxide (Electron Microscopy Sciences), rinsed, scraped up with a rubber policeman, centrifuged, and embedded with Spurr Resin (Polysciences, Inc., Warrington, PA) according to the manufacturer's specifications. Thick sections were visualized at 300 keV in a Phillips CM-30 (Phillips Scientific, Mahwah, NJ) IVEM and photographed as stereo pairs. Serial thin sections were also cut from these blocks.

Results

Localization of β-VLDL with LAMP-1

Because LDL degradation occurs in acidic lysosomes in macrophages, it was important to determine whether the peripheral β-VLDL was in degradative organelles. We addressed this issue by determining if immunofluorescence labeling with LAMP-1, a late endosome–lysosome marker (Hughes and August, 1981), colocalized with DiI-β-VLDL. Before immunofluorescence staining, macrophages were incubated at 37°C with DiI-β-VLDL for 5 min, unbound ligand was rinsed away, and the cells were chased in the absence of ligand for 5 min, at 37°C. As in our earlier studies (Tabas et al., 1990, 1991) this resulted in delivery to both peripheral and perinuclear β-VLDL containing compartments. A similar distribution of β-VLDL was observed after immunofluorescence staining (Fig. 1 *A*), although some DiI label was lost during cell permeabilization. The LAMP-1 staining (Fig. 1 *B*) revealed a largely perinuclear distribution of the antigen, with some lightly labeled compartments in the cell periphery. In addition, LAMP-1 was found in linear or curvilinear elements, presumably tubular lysosomes. While many of the perinuclear compartments containing β-VLDL were LAMP-1 positive, the peripheral β-VLDL compartments stained for LAMP-1 only rarely, and β-VLDL did not colocalize with the tubular lysosomes. Virtually all of the LDL-containing compartments in macrophages were positive for LAMP-1 (not shown). These results suggested that the peripheral β-VLDL was not in a degradative compartment, or at least not in late endosomes/lysosomes. We then considered another important factor in ligand degradation: whether the widely distributed β-VLDL-containing compartments were acidic.

Characterization and Endocytic Distribution of Fluorescein-labeled β-VLDL

Fluorescein-labeled molecules can be used for ratiometric measurements of pH (Maxfield, 1989). Thus, we labeled β-VLDL with FPE and characterized its endocytic processing in macrophages. Fig. 2 compares the endocytic distribution of Texas red (TR)–labeled α-2-macroglobulin (α_2M) (Fig. 2 *A*) with that of FPE-β-VLDL (Fig. 2 *B*). The macrophages were incubated with FPE-β-VLDL and TR-α_2M for 6 min at 37°C, followed by 4 min at 37°C in the absence of ligand. α_2M, like LDL, is rapidly targeted to perinuclear lysosomes (Fig. 2 *A*) and serves as a convenient marker for lysosomal targeting in macrophages (Tabas et al., 1991). Some FPE-β-VLDL (Fig. 2 *B*) colocalized with α_2M in perinuclear compartments, but a significant amount of the lipoprotein was distributed throughout the cell. This distribution of FPE-β-VLDL was indistinguishable from that of DiI-β-VLDL seen in previous studies (Tabas et al., 1990, 1991) in which the peripheral β-VLDL represented 40–60% of the total cell-associated β-VLDL. Uptake of FPE-β-VLDL was competed by a 50-fold excess of unlabeled β-VLDL, and incubation of FPE-β-VLDL with an excess amount of anti-apoE antibody also resulted in loss of binding and uptake by the macrophages (data not shown). These results indicated that FPE-β-VLDL was binding to the LDL receptor on macrophages (the apo-B,E receptor) and was an appropriate probe for measurement of pH during β-VLDL endocytic processing.

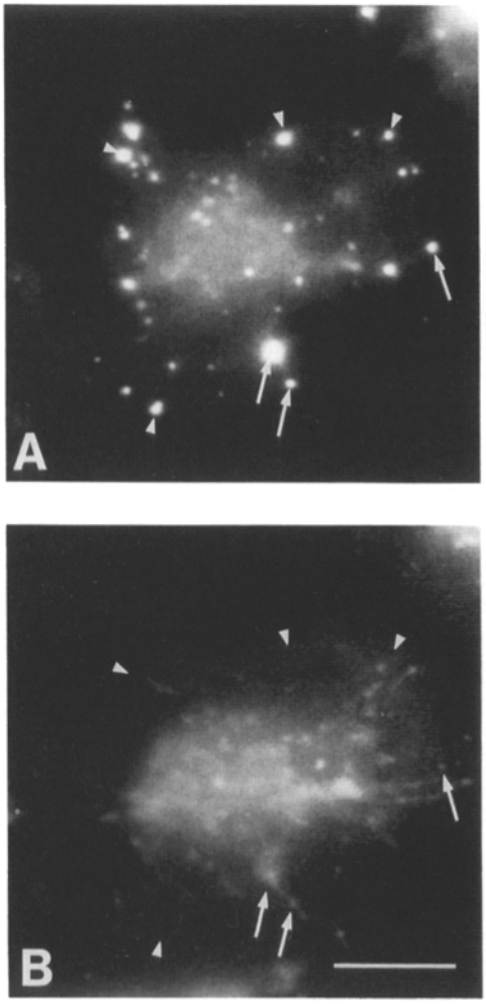

Figure 1. Immunofluorescence microscopy of macrophages incubated with DiI–β-VLDL and labeled for LAMP-1. Macrophages were incubated with DHB containing DiI-labeled rabbit β-VLDL (5 μg/ml) for 5 min at 37°C and then chased in the absence of ligands at 37°C for 5 min. The cells were fixed and immunofluorescence labeled as described in the Materials and Methods. Images were recorded using a cooled CCD camera. *A* shows the DiI–β-VLDL labeling in cells processed for immunofluorescence, and *B* shows the anti–LAMP-1 staining of the cells shown in *A*. Arrows indicate examples of compartments that appeared to colocalize with LAMP-1 labeling, and arrowheads indicate compartments that contained only β-VLDL. Bar, 10 μm.

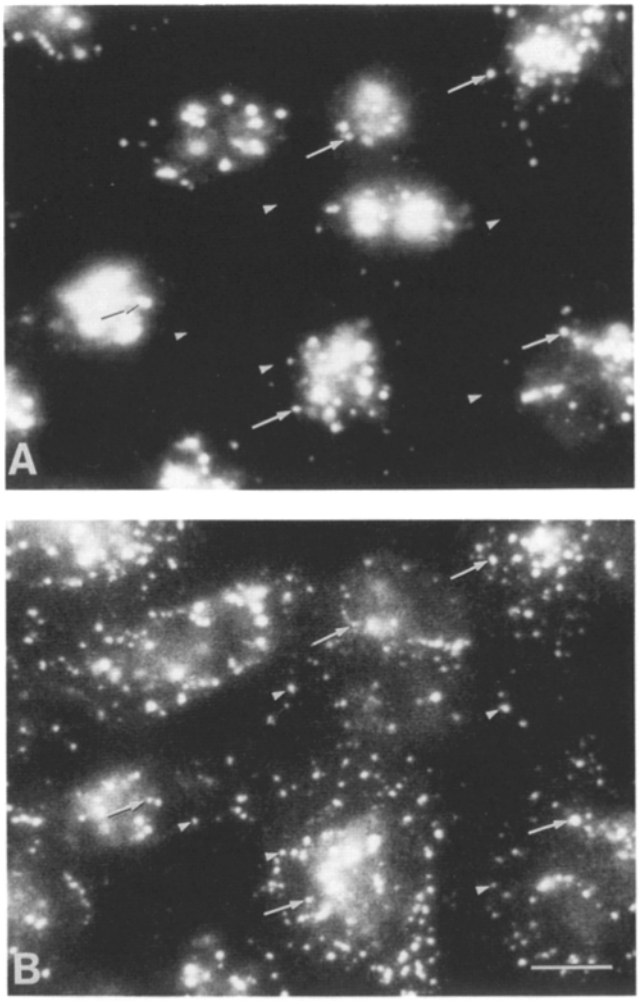

Figure 2. Fluorescence microscopy of macrophages incubated with FPE–β-VLDL and TR-α_2M. Macrophages were incubated with DHB containing TR-α_2M (75 μg/mL) and FPE–β-VLDL (5 μg/mL) for 6 min at 37°C and then chased in the absence of ligands at 37°C for 4 min. The cells were then fixed and viewed by fluorescence microscopy, and images were recorded using a cooled CCD camera. TR-α_2M is shown in *A*, and the corresponding FPE–β-VLDL labeling is shown in *B*. Examples of compartments that contain both α_2M and β-VLDL are indicated with arrows, and widely distributed β-VLDL compartments are indicated with arrowheads. Bar, 10 μm.

pH of Compartments Containing FPE-β-VLDL

Using FPE–β-VLDL, we performed ratiometric measurements of pH in living macrophages after a 5-min pulse at 37°C with ligand, and a 5-min chase at 37°C in the absence of ligand. Fluorescein fluorescence ratios using two excitation wavelengths were measured as described in Materials and Methods, and a TR-α_2M image was also recorded for each field of cells. Compartment pHs were assigned by comparing ratios measured in living cells to a standard curve generated using permeant buffers of known pH in fixed cells. Fig. 3 shows the distribution of pHs of β-VLDL containing compartments in living macrophages; the standard curve is inset. This distribution is notable for the large fraction of compartments found at either neutral (≥7.0) or highly acidic (≤5.5) pH. In addition, comparison of the FPE–β-VLDL images with the TR-α_2M image revealed that virtually none of the peripheral compartments were acidic, while the perinuclear, TR-α_2M containing compartments were highly acidic. The low pH of the perinuclear compartments was confirmed by other pH measurements using fluorescein-α_2M (F-α_2M) and DiI–LDL (not shown), in which the perinuclear, LDL containing compartments, which colocalized with F-α_2M, were highly acidic.

The existence of many neutral (pH ≥7.0) compartments was surprising since endosomes in many cell types are acidified within <5 min (Maxfield and Yamashiro, 1991). Because the 450/490 ratio varies slowly above pH 7 (Fig. 3,

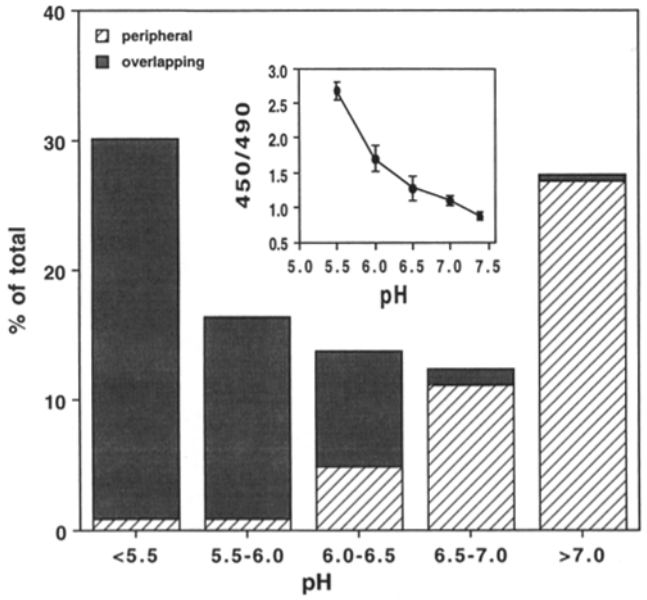

Figure 3. pH measurements using FPE–β-VLDL. Macrophages were incubated with DHB containing FPE–β-VLDL (5 μg/mL) for 5 min at 37°C, rinsed with 37°C DHB, and then chased in DHB in the absence of ligands at 37°C for 5 min. The cells were rinsed with normal saline solution, and images were recorded and analyzed as described in Materials and Methods. β-VLDL containing compartments that were colocalized with α_2M were assigned to the overlapping category, and all others were considered peripheral. The stacked bars show the contribution of each type of compartment to the total percentage of β-VLDL found in a given pH range. The inset shows the pH dependence of the 450/490 ratios determined with fixed cells under the conditions of the live cell experiment. Error bars = SEM, N > 150 except pH 5.5, where N = 81.

inset), we could not determine whether these high pH compartments were at the extracellular pH. Thus it was necessary to determine by independent means whether the peripheral β-VLDL–containing compartments were accessible to the external medium.

Accessibility of β-VLDL Compartments to a Fluorescence Quencher

To determine if the peripheral β-VLDL–containing compartments were accessible to the extracellular medium, we took advantage of the fact that trypan blue, which does not penetrate intact lipid bilayers (Golan et al., 1986), quenches fluorescein fluorescence (Weersink et al., 1990; Hed et al., 1987). After a 6-min pulse at 37°C and a 4-min chase at 37°C in the absence of ligand, we added trypan blue to the solution bathing the living macrophages, recording the image before and immediately after trypan blue addition. Virtually all of the peripheral β-VLDL was accessible to the quencher (Fig. 4). Before trypan blue addition the cells exhibited an endocytic pattern shown in Fig. 4 *A*, with FPE–β-VLDL in both perinuclear lysosomes and peripheral compartments. In Fig. 4 *B*, immediately after trypan blue addition (within 1–2 s) the fluorescence signal from the widely distributed FPE–β-VLDL virtually disappeared, and the pattern of the remaining β-VLDL closely resembled the perinuclear distribution of TR-α_2M, shown in Fig. 4 *C*.

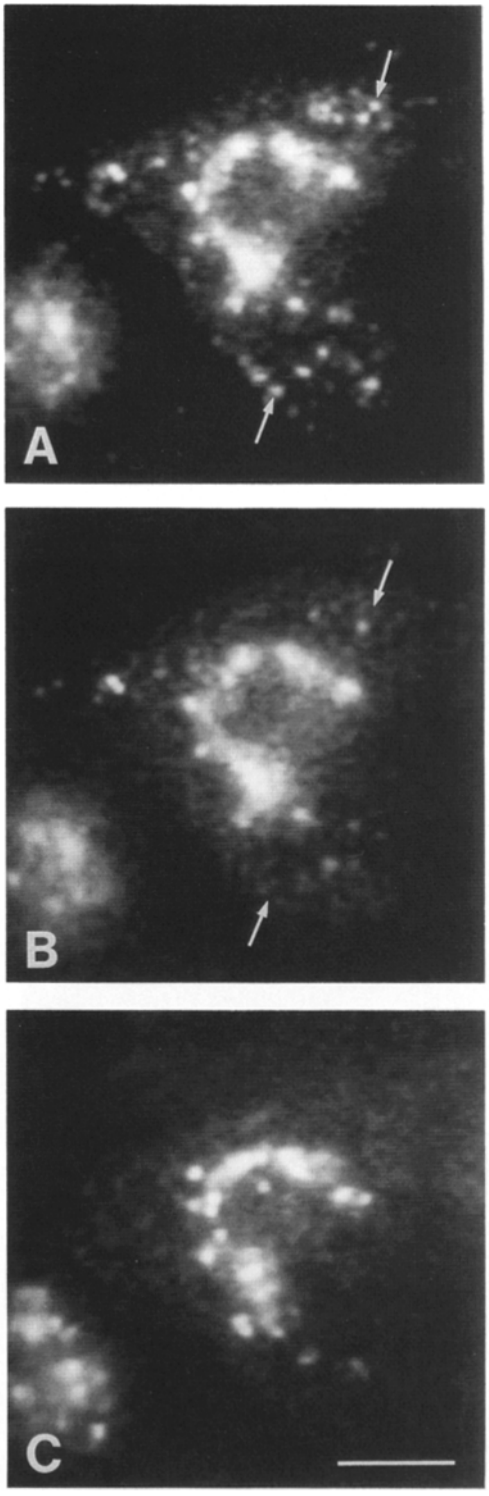

Figure 4. Quenching of FPE-β-VLDL fluorescence by trypan blue in living macrophages. Macrophages were incubated with DHB containing FPE–β-VLDL (5 μg/mL) and TR-α_2M (75 μg/mL) for 6 min at 37°C and then chased in the absence of ligands at 37°C for 4 min. The cells were then rinsed with normal saline solution, and after addition of methylamine (final concentration, 10 mM), viewed using video intensification enhanced fluorescence microscopy. FPE–β-VLDL is shown (*A*) before and (*B*) after addition of trypan blue to 2 mg/mL. The corresponding TR-α_2M image is shown in *C*. Arrows indicate examples of β-VLDL compartments that were quenched. Bar, 10 μm.

Under the same pulse–chase conditions fluorescein-labeled α_2M was completely unaffected by trypan blue addition (not shown). pH measurements of β-VLDL compartments after trypan blue addition revealed almost exclusively acidic compartments.

Previously we showed that <10% of cell-associated β-VLDL was suramin releasable after a 10-min pulse and 5-min chase (Tabas et al., 1990). However, quenching experiments with trypan blue reflect access of a small molecule (≈1,000 D) to the β-VLDL compartment, while the suramin experiment measured the release of a large particle (β-VLDL) from the cell. We therefore investigated whether the β-VLDL compartment was accessible to macromolecules in the extracellular space.

β-VLDL Compartments Are Partially Accessible to Antibodies

To determine whether the widely distributed β-VLDL compartment was accessible to macromolecules in the extracellular space, we labeled fixed, nonpermeabilized macrophages by immunofluorescence using anti-apoprotein E (apoE) antibody (Fig. 5). When the cells were surface labeled with DiI–β-VLDL and then fixed at 4°C, all of the β-VLDL could be labeled with anti-apoE. A few of the double-labeled particles are indicated by arrows as in Fig. 5, *A* (DiI–β-VLDL) and *B* (anti-apoE). In contrast, if a 5′ pulse and 5′ chase experiment at 37°C was carried out before immunofluorescence labeling, some β-VLDL bound the anti-apoE, as indicated by the arrows in Fig. 5, *C* (DiI–β-VLDL)

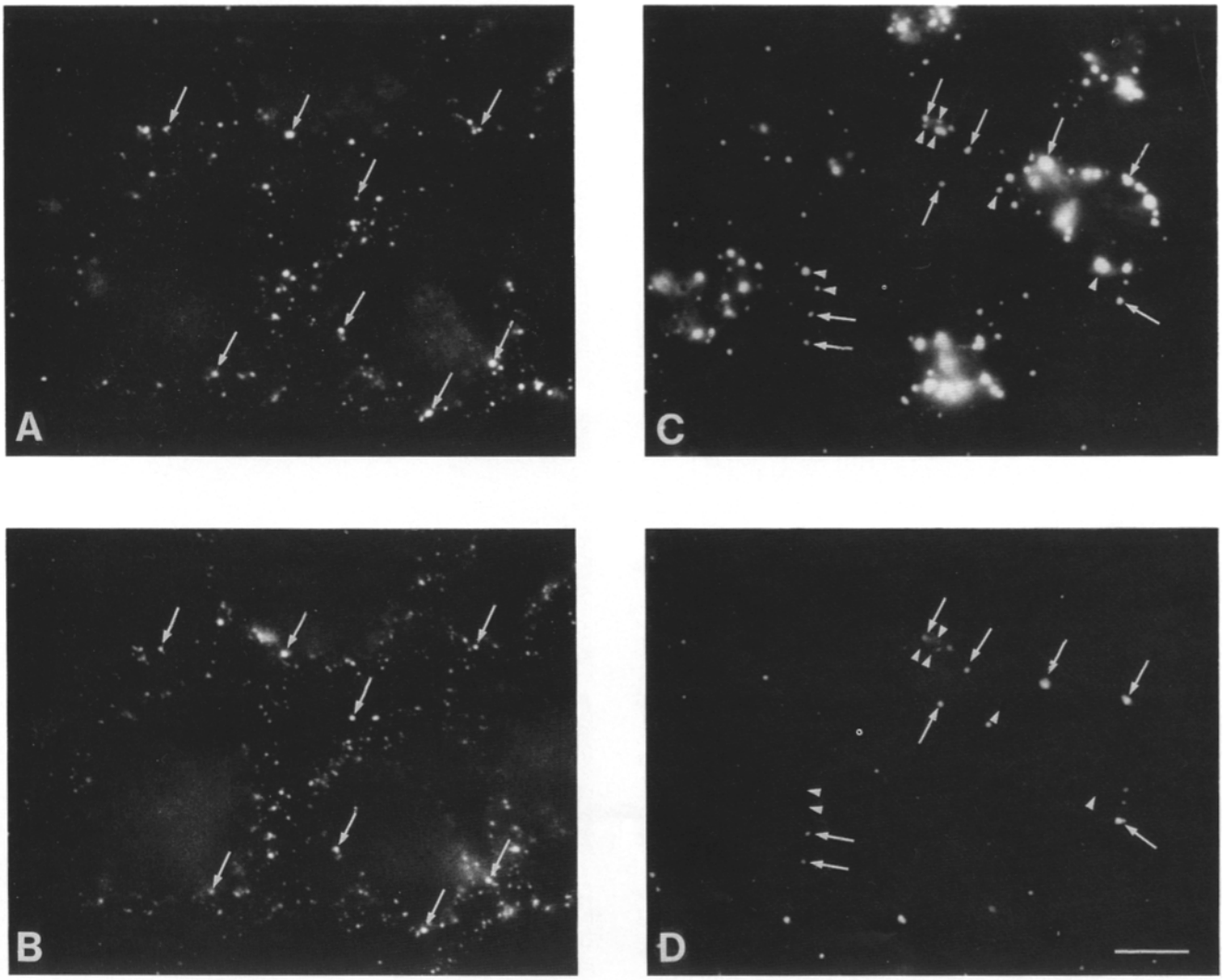

Figure 5. Macrophages incubated with DiI–β-VLDL and labeled for surface apoE. In *A* macrophages were incubated with DHB containing DiI–β-VLDL (5 μg/ml) at 4°C for 30 min, while in *C* cells were incubated at 37°C for 5 min and chased in the absence of ligand for 5 min at 37°C. Both samples were fixed and processed for immunofluorescence (without permeabilization) as described in Materials and Methods. The anti-apoE labeling corresponding to the cells in *A* and *C* is shown in *B* and *D*, respectively. Arrows indicate examples of β-VLDL compartments that labeled with anti-apoE, and arrowheads indicate some compartments that did not label with anti-apoE. Images were recorded using a cooled CCD camera. Bar, 10 μm.

and *D* (anti-apoE). However, many β-VLDL compartments, including peripheral compartments, could not be labeled with anti-apoE (Fig. 5, *C* and *D*, *arrowheads*).

In additional experiments, we determined whether the peripheral β-VLDL–containing compartments were accessible to AFA (Salzmann and Maxfield, 1988), which like trypan blue, quenches fluorescein fluorescence. However, AFA is much larger than trypan blue, allowing us to determine, in living cells, whether there were size limitations to accessibility to the compartment. FPE is laterally mobile in membranes into which it is incorporated (Foley et al., 1986) and should be randomly distributed about the surface of the β-VLDL. Using fixed cells that had been labeled with FPE–β-VLDL at 4°C for 30 min, quenching of FPE–β-VLDL by the antibody occurred within seconds, to ~50% of the initial intensity (not shown). In living cells incubated at 37°C for 5 min with FPE–β-VLDL and chased for five additional minutes, some widely distributed compartments were quenched by both AFA and trypan blue, but most were quenched only by trypan blue (not shown). This result, along with the anti-apoE immunofluorescence, suggested that macromolecules had limited access to β-VLDL compartments that were fully accessible to small molecules.

Kinetics of Loss of Accessibility of β-VLDL Compartments to a Fluorescence Quencher

After long chase times (>10 min) most of the β-VLDL could be found in the perinuclear region of the cell (see below). To determine if the amount of β-VLDL accessible to trypan blue would decrease over time, FPE–β-VLDL was bound to macrophages at 4°C for 30 min, unbound lipoprotein was rinsed away, and the cells were incubated at 37°C in the absence of lipoprotein for various times. The fraction of the total cell-associated FPE–β-VLDL that was quenched by trypan blue was measured at each time point (Fig. 6). The half-time for loss of accessibility to trypan blue was ~6 min, and all of the accessible FPE–β-VLDL was in peripheral compartments. In contrast, after a 4-min chase, LDL was found exclusively in perinuclear compartments that colocalized with F-α_2M, and the F-α_2M was completely unaffected by trypan blue addition (not shown). The kinetics of FPE–β-VLDL accessibility to trypan blue were not influenced significantly by cooling the cells for ligand binding. If a short (3–5 min) incubation with FPE–β-VLDL was carried out at 37°C rather than binding in the cold, the half-time was unchanged, but with a lower trypan blue accessibility at the beginning of the chase, because some β-VLDL was internalized during the pulse. These experiments showed that the peripheral, trypan blue–accessible β-VLDL compartments were not permanent but represented an early stage in the processing of β-VLDL.

Progression of Peripheral β-VLDL Compartments to the Perinuclear Region

To observe the dynamics of β-VLDL processing in macrophages we used time-lapse video intensification microscopy. After a 6-min pulse with DiI–β-VLDL at room temperature (~21°C), the cells were chased in the absence of ligand on the microscope stage at 37°C. Fig. 7 tracks two compartments over a 100 second period. The β-VLDL compartments exhibited limited motion while in the cell periphery (compartments 1 and 2), but after initiating movement they proceeded rapidly and unidirectionally to the perinuclear region of the cell (compartment 2). Every β-VLDL compartment moved toward the perinuclear region, and the average velocity was ~0.25 μm/s, consistent with microtubule motor-based locomotion (Dabora and Sheetz, 1988). Some compartments appeared to increase significantly in brightness while in the cell periphery (compartment 1), suggesting that β-VLDL accumulated in these compartments. Independent experiments have shown that after long chase times (>10 min) virtually all of the β-VLDL colocalizes with α_2M in lysosomes (not shown).

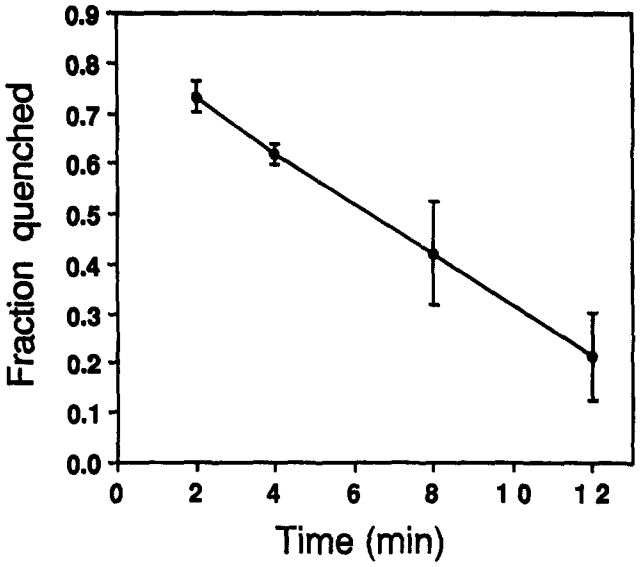

Figure 6. The kinetics of loss of accessibility of FPE–β-VLDL to trypan blue. Macrophages were incubated with DHB containing FPE–β-VLDL (5 μg/mL) for 30 min at 4°C, rinsed with 37°C DHB, and then chased in DHB in the absence of ligands at 37°C for 2, 4, 8, or 12 min. The cells were rinsed with normal saline solution, and methylamine was added (final concentration, 10 mM). Images were acquired both before and immediately after trypan blue addition to 2 mg/mL, and processed as described in Materials and Methods. Each field of cells was analyzed for the fraction of the total amount of FPE–β-VLDL that was accessible to trypan blue. Each time point represents an average of either three or four fields; bars, standard deviations.

Electron Microscopic Characterization of β-VLDL Compartments

The results to this point suggested that β-VLDL was internalized into a compartment that was to some degree accessible to the extracellular space. To determine the ultrastructural properties of the widely distributed β-VLDL compartment, cells were incubated with ^{125}I–β-VLDL and processed for EM using the tannic acid/para-phenylene diamine procedure of Guyton and Klemp (1989), which preserves the structure of lipoprotein particles. Thus, in EM autoradiograms of these cells, β-VLDL could be visualized as small circular structures, some of which were labeled with autoradiographic grains. Fig. 8 shows representative EM autoradiograms of macrophages that were incubated with ^{125}I–β-VLDL for 6 min, followed by either no chase (Fig. 8 *A*) or a 2-min chase at 37°C (Fig. 8 *B*). With no chase (Fig. 8 *A*) some β-VLDL could be observed on the cell surface, alone or in

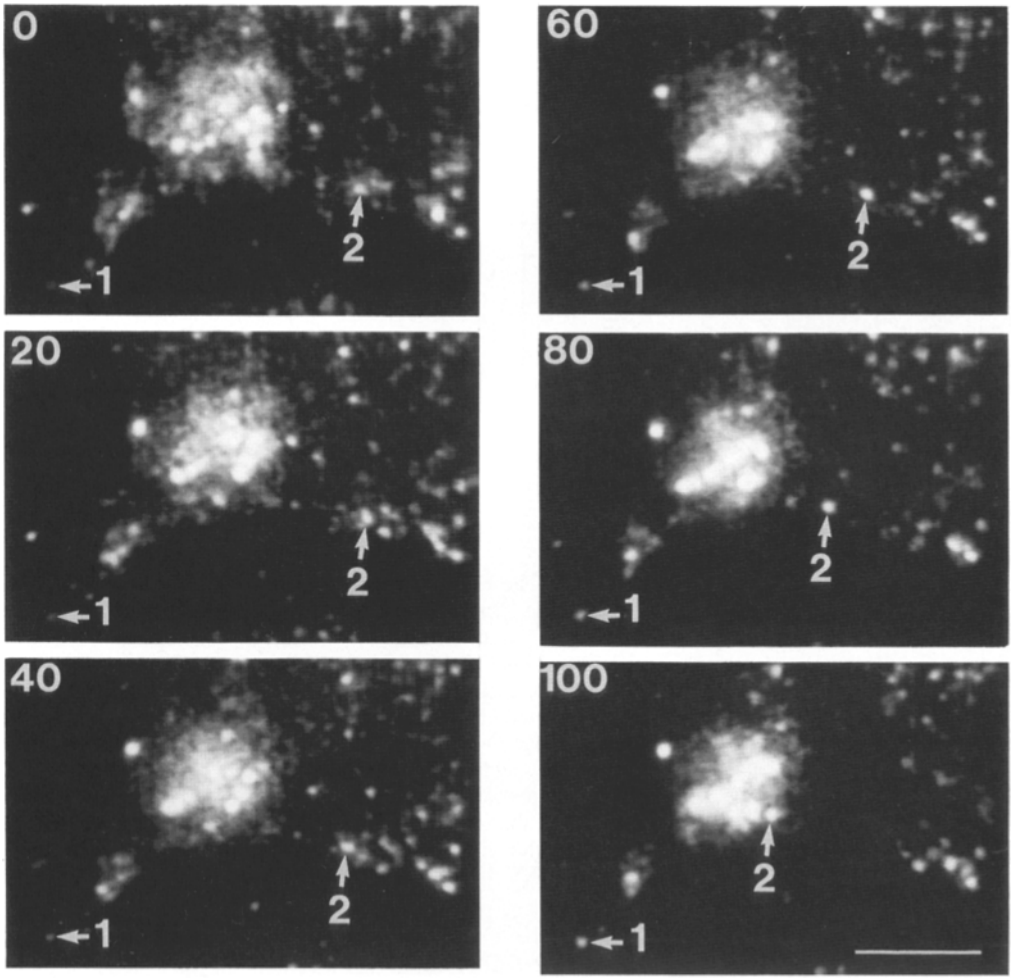

Figure 7. Progression of β-VLDL from the periphery to the perinuclear region of the cell. Macrophages were incubated with DiI–β-VLDL (10 μg/mL) for 6 min at room temperature and chased at 37°C on a heated microscope stage. Images were recorded every 10 s for the next 10 min. The sequence shown here starts 50 s after warm-up to 37°C, and shows frames separated by 20 s. Two compartments are followed from frame to frame, each compartment specified with a number. Bar, 10 μm.

small clusters. In addition, some β-VLDL was found associated with coated regions of the plasma membrane, presumably clathrin-coated pits (not shown). After a 2-min chase, virtually none of the β-VLDL particles were found on the cell surface (Fig. 8 *B*). The β-VLDL–containing compartments (Fig. 8 *B*) were electron-lucent, frequently located close to the plasma membrane, and often contained multiple β-VLDL particles. These electron-lucent structures ranged in size from ~250 to 600 nm. In none of these images, though, were we able to observe direct connection(s) to the extracellular space from internal structures.

Because thin sectioning often obscures the continuity of tubular or reticular structures, we used IVEM of thick sections (0.3–0.5 μm) to provide a more complete view of the structure of the peripheral β-VLDL compartments. We labeled DiI–β-VLDL with 26-nm colloidal gold and determined that the specificity of binding and endocytic pattern of the β-VLDL–gold was the same as that of native β-VLDL. Macrophages were incubated for 6 min with β-VLDL–gold at 37°C, chased for 4 min at 37°C in the absence of ligand, fixed, scraped from the dish, centrifuged, and processed for thick section IVEM. Fig. 9, *A* and *B* show stereo pairs of cells in which β-VLDL can be seen at the end of tubules that lead to the cell surface. These tubules were ~250 nm in diameter, and were often >1 μm in length. Tubules of similar dimensions were also observed in cells incubated without β-VLDL. In all of the micrographs examined thus far, β-VLDL appeared at or near the end of the tubule, farthest from the cell surface. In serial thin sections of the same preparations, coated regions of membrane have been observed at the plasma membrane and along the tubules (not shown), but as yet none have been observed at the base of the tubules where the β-VLDL was found. A few of these thin sections also showed β-VLDL in a tubule with a continuous opening to the surface (Fig. 9 *C*). In thin sections through pelleted cells, the sections are cut at random orientations, whereas the EM autoradiography sections were cut parallel to the cell monolayer. IVEM of the whole mounts of cells incubated with β-VLDL–gold indicated that the tubules were at an angle to the substrate (not shown) so that the autoradiography sections would have cut cross-sections through the tubules.

In addition to revealing the structure of the peripheral β-VLDL compartment, these experiments demonstrated the continuity of the compartment with the plasma membrane. Thus, the predominant form of peripheral β-VLDL containing compartments in these preparations appeared to be a

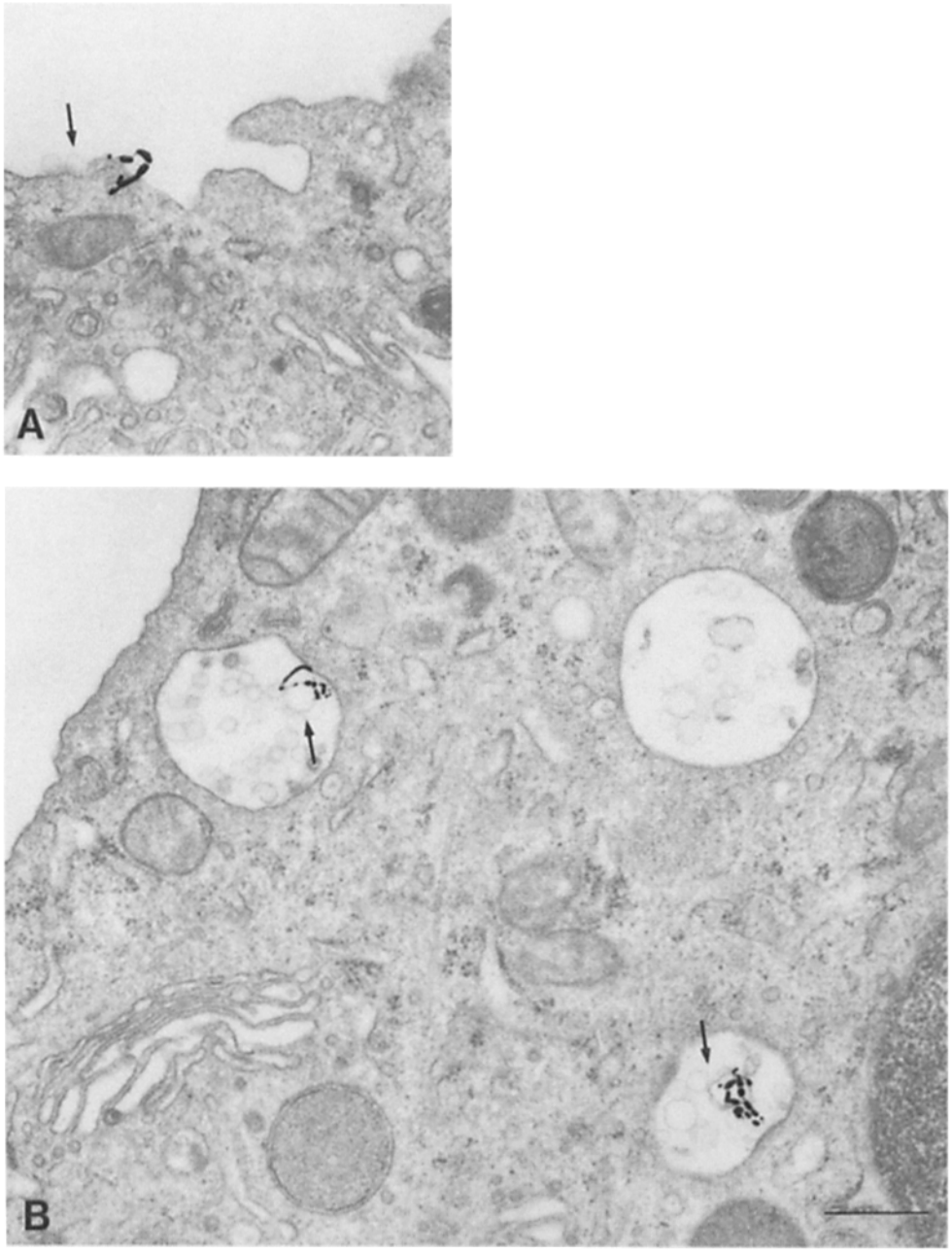

Figure 8. Electron microscopic autoradiography of ^{125}I–β-VLDL. Macrophages were incubated with ^{125}I–β-VLDL (10 μg/mL) for 6 min at 37°C, followed by either (*A*) no chase, or (*B*) a 2-min chase at 37°C in the absence of ligand. After fixation, treatment with tannic acid and paraphenylenediamine, and embedding, thin sections were prepared and exposed for autoradiography for 4 wk before viewing. Representative β-VLDL particles are highlighted with arrows. Bar, 500 nm.

long tubule with one or more β-VLDL residing at the base of the structure.

Degradation of β-VLDL in the Peripheral Compartments

Cholesterol delivery by lysosomal hydrolysis of lipoproteins can stimulate ACAT activity in macrophages (Brown et al., 1975; Goldstein et al., 1980). To determine whether β-VLDL was undergoing degradation or processing in the peripheral compartments, we used fluorescence resonance energy transfer (FRET) microscopy (Herman, 1989; Uster and Pagano, 1986) to assess the integrity of the β-VLDL. Using β-VLDL labeled with both donor (C18-DiO) and acceptor (C18-DiI) fluorescent lipid analogs, in intact particles we observed significant donor quenching (detected as low donor to acceptor fluorescence ratios) in solution in a fluorometer, or on cell-free substrates in the fluorescence microscope (not shown). Changes in the integrity of the β-VLDL that separate DiI from DiO will relieve the donor quenching caused by fluorescence resonance energy transfer, since the efficiency of FRET falls as the sixth power of the distance between donor and acceptor (Herman, 1989). FRET of DiO–DiI–β-VLDL was stable in the presence of albumin or liposomes at 37°C, but in the fluorometer addition of detergent to disrupt the lipoproteins resulted in a 2–5-fold increase in the donor:acceptor fluorescence ratio.

Incubation of CHO fibroblasts with DiO–DiI–β-VLDL for

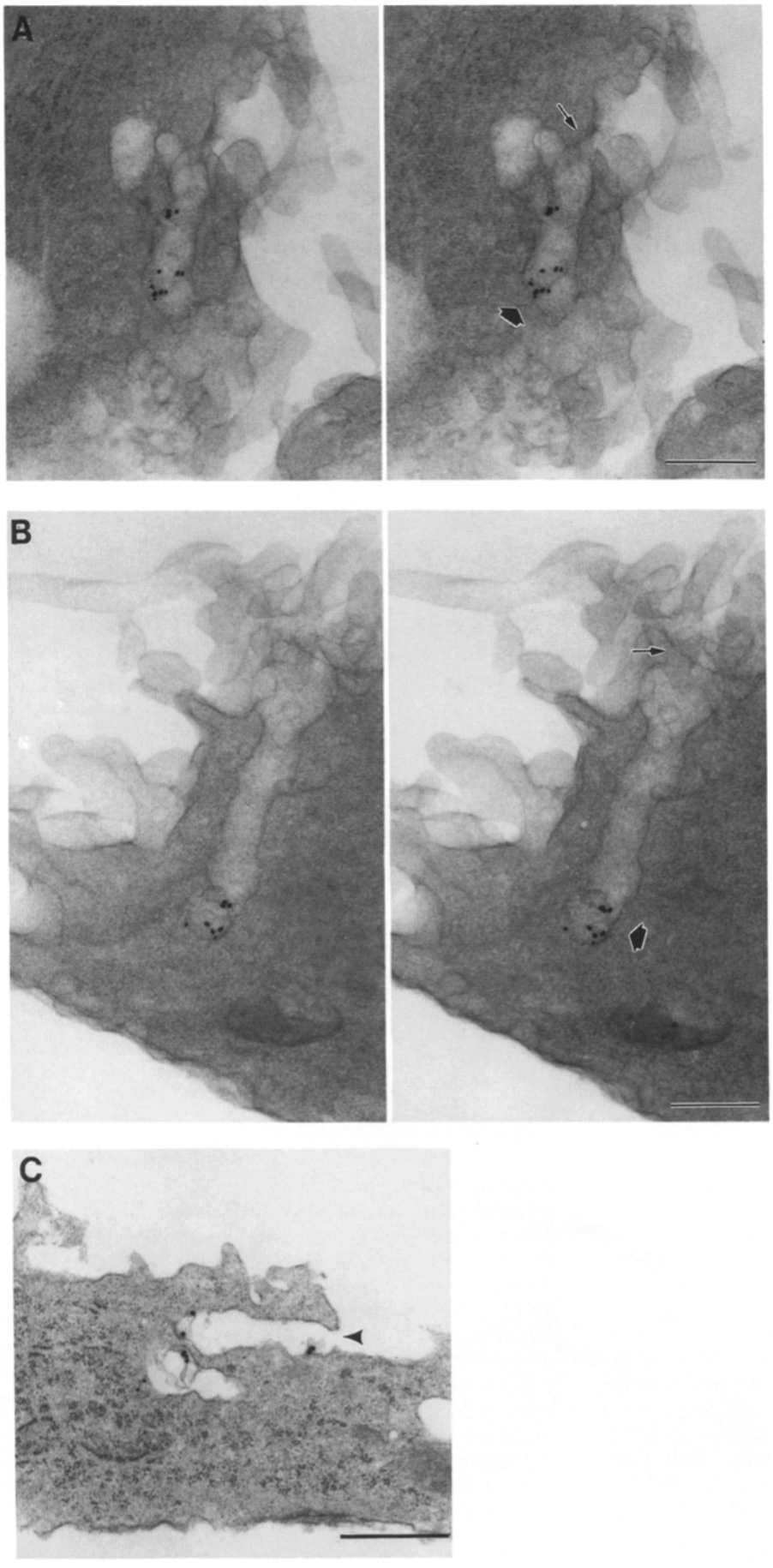

Figure 9. Electron microscopy of colloidal gold-labeled β-VLDL interactions with macrophages. Cells were incubated with 26-nm colloidal gold–β-VLDL (3 μg/mL) for 6 min at 37°C, followed by a 4 min chase at 37°C in the absence of ligand. Cells were fixed and processed for EM as described in Materials and Methods. *A* and *B* show two different stereo pairs of thick sections containing tubular β-VLDL compartments. Thick sections (0.3–0.5 μm) were visualized at 300 keV in a Phillips CM-30 IVEM and photographed as stereo pairs. The opening to the extracellular space is indicated with a small arrow, and gold particles are highlighted with a wide arrow. *C* shows a thin section which included a tubular profile containing β-VLDL. Adjacent serial sections (not shown) indicate that this is a tubule with dimensions similar to those shown in *A* and *B*. Bar, 500 nm.

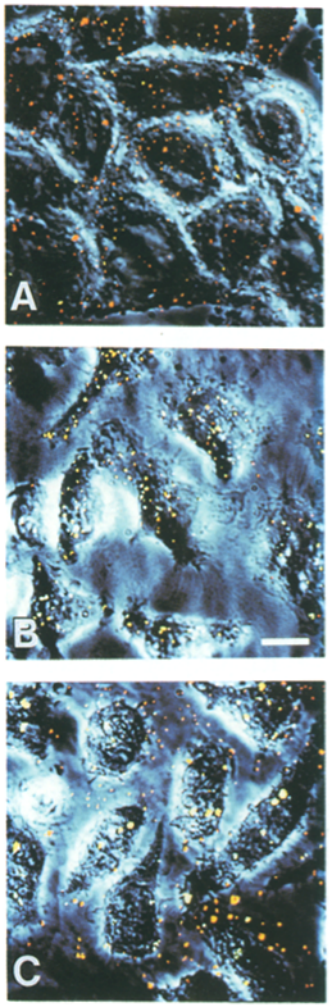

Figure 10. Degradation of β-VLDL in peripheral compartments. CHO cells (*A*) or mouse peritoneal macrophages (*B*) were incubated with DiI–DiO–β-VLDL, 10 μg/mL for 5 min at 37°C, followed by a chase in the absence of ligand, for 2 min at 37°C. The cells in *C* were mouse peritoneal macrophages incubated with 10 μg/mL double-labeled β-VLDL for 30 min on ice, and fixed on ice. Shown superimposed on the phase-contrast image of each field of cells is a pseudocolor representation of the ratio of green (DiO) to red (DiI) fluorescence calculated for each particle. Low ratios are shown in red, while orange to yellow to green compartments represent progressively higher ratios. Samples were fixed in 4% formaldehyde for 5 min (except for C; 10 min on ice) and immediately viewed. Images were recorded using a cooled CCD camera, and processing was as described in Materials and Methods. Bar, 10 μm.

5 min at 37°C followed by a 2-min chase at 37°C in the absence of ligand indicated that no loss of FRET had occurred, as indicated by the red dots in Fig. 10 *A*. In contrast, with macrophages, a loss of integrity of the DiO–DiI–β-VLDL was observed after a 5-min pulse at 37°C with DiO–DiI–β-VLDL, and a 2-min chase at 37°C in the absence of ligand, shown by the yellow dots in Fig. 10 *B*, identical conditions as the fibroblast experiment. Many of the β-VLDL structures showing loss of FRET were in the periphery of the cell, and we know that under the conditions of this experiment nearly all of the peripheral β-VLDL is in surface tubules. As further confirmation of the ability of macrophages to process β-VLDL at the plasma membrane, we incubated macrophages with DiO–DiI–β-VLDL for 30 min on ice, followed by fixation on ice, and observation within ten minutes after warming to room temperature. As shown in Fig. 10 *C* this resulted in noticeable loss of integrity for some of the DiO–DiI–β-VLDL. Thus it appears that some activity is present on the macrophage surface, and in the tubules that contain peripheral β-VLDL, that can significantly disrupt the integrity of β-VLDL.

Discussion

The experiments presented here demonstrate an unusual endocytic mechanism for the uptake of β-VLDL into mouse peritoneal macrophages. The results show that β-VLDL is transiently sequestered into a tubular compartment that is removed from the cell surface but open to the external milieu. Some degradation of the peripheral β-VLDL occurs, and the lipoprotein then enters a fully sealed compartment, with a half-time of ~6 min. After internalization, the β-VLDL is rapidly delivered to perinuclear lysosomes. IVEM of 0.3–0.5-μm sections provides a clear visualization of the peripheral structures, and digital fluorescence microscopy provides quantitative data on their dynamic properties.

Several lines of evidence showed that β-VLDL is sequestered from the cell surface within 2–4 min after binding. Few β-VLDL particles bound anti-apoE or anti-fluorescein antibody after a 2–4-min chase, while β-VLDL bound to the cell surface at 4°C was always accessible to the antibodies. In addition, our previous work had shown that only ~10% of the β-VLDL was releasable by suramin under these conditions (Tabas et al., 1990). Rapid-freeze deep-etch electron micrographs were consistent with these observations: at 4°C β-VLDL could be found on both flat and concave regions of membrane (probably coated pits), but after a 6-min pulse and 4-min chase at 37°C very little β-VLDL was visible on the cell surface (Myers, J., I. Tabas, F. Maxfield, and R. G. W. Anderson, unpublished data). Finally, EM autoradiography of thin sections confirmed that β-VLDL was removed from the cell surface, and appeared in electron lucent structures ~250–600 nm in diameter. It was clear from these observations that the peripheral β-VLDL was not merely adherent to the cell surface, but must be removed from the cell surface in some way.

The first indication that the peripheral β-VLDL–containing compartments might be accessible to the cell surface was the high percentage of compartments that were not acidic. Endosomes acidify rapidly after internalization (Tycko and Maxfield, 1982; Maxfield and Yamashiro, 1991), and after a 4- or 5-min chase none of the β-VLDL compartments should have been found at a neutral pH. The rapid (1–2 s) quenching of the fluorescence of widely distributed FPE–β-VLDL by trypan blue dramatically confirmed that these peripheral compartments have an opening to the cell surface. However, the poor accessibility to antibodies suggested that access to the compartment was restricted.

We were unable to obtain evidence for connections to the cell surface in thin section EM autoradiograms. The electron-lucent structures could either be cross sections of tubules or fully sealed vesicles being transported to the central region of the cell. However, in 0.3–0.5-μm sections, we observed clear connections between the widely distributed β-VLDL and the cell surface. The large-diameter (200–250 nm) tubular connections to the cell surface shown here were seen frequently in these cells, consistent with the large fraction of β-VLDL that was accessible to trypan blue under the same conditions. These electron micrographs also illustrate the often tortuous path connecting β-VLDL compartments with the cell surface. The long, convoluted structure of these tubules probably accounts for the poor accessibility to antibodies. It is also evident that thin sectioning could obscure the connections to the surface.

These tubules are unusual endocytic structures. Coated regions of membrane were found along the tubules but not at the ends where β-VLDL accumulated preferentially. However, the fraction of β-VLDL that binds to coated pits, and

the efficiency with which it is internalized, was not determined in our experiments. Deeply invaginated coated pits have been observed in fibroblasts (Pastan and Willingham, 1981), but the tubules connecting these coated pits to the cell surface were quite narrow (<100 nm), and the coated membrane was always at the end of the tubule. It seems likely that some internalization of β-VLDL involves clathrin-coated pits, but the relatively slow kinetics of internalization and the lack of colocalization with coated membrane argue against conventional coated pit endocytosis for the β-VLDL that enters macrophages via surface tubules.

Macrophages are a pinocytically active cell type, and Nichols (1982) observed tubules connecting pinocytic vesicles with the cell surface. However, these tubules were only 30–60 nm in diameter, and they were <1 μm in length. Tubules connected to the cell surface were also observed in macrophages during Fc receptor-mediated frustrated phagocytosis (Bainton et al., 1989), but these tubules, like those described above, were very thin (50–80 nm) compared with the tubules described in this report. Macropinosomes, which occur frequently in stimulated macrophages (Swanson et al., 1989), result in the internalization of large volumes of extracellular fluid into sealed compartments. This differs markedly from our observations, which indicate that little fluid is co-internalized with β-VLDL (not shown). The tubular structures containing β-VLDL also do not seem similar to the initial steps in phagocytosis. In none of our experiments does the membrane surrounding β-VLDL appear to be closely apposed to a single β-VLDL particle, as it would be in phagocytic uptake (Griffin et al., 1975). We also know from quantitative microscopy that some accumulation of β-VLDL occurs in the peripheral compartment, while it is still trypan accessible, again inconsistent with phagocytosis. The tubules are not tubular lysosomes, since they are LAMP-1 negative and neutral in pH. Similar tubules are seen in cells that were not incubated with β-VLDL, indicating that these structures may not be ligand-induced. However, it is difficult to quantify the number of tubules per cell since even in thick sections the tubules frequently extend beyond a single section. Further characterization of the peripheral β-VLDL compartment should help to determine its structure and composition.

The half-time for entry of β-VLDL into fully sealed compartments was determined by fluorescence quenching experiments to be ~6 min. We could not use the IVEM of thick sections for quantitative studies of internalization since the continuity with the surface was ambiguous for tubules which extended beyond the section. However, each of the EM studies showed that nearly all of the β-VLDL was cleared from open areas of the cell surface within 2–4 min. The predominant peripheral localization of β-VLDL–gold after a 6-min incubation and 4-min chase was tubules similar to those shown in Fig. 9. The amount of β-VLDL–gold seen in tubules would be consistent with the fraction of β-VLDL that remains sensitive to trypan blue (Fig. 6). Our interpretation is that the trypan blue–sensitive β-VLDL is in these deep tubules.

We do not know whether entire tubules seal or if vesicles bud off from them. However, time-lapse video microscopy indicates that all of the β-VLDL at the end of a tubule stays together when it becomes fully internalized. Once the vesicles pinch off, they move rapidly to the center of the cell. After 10–20 min β-VLDL is found in highly acidic, LAMP-1 positive organelles, consistent with its eventual degradation in the lysosomes of these cells (Tabas et al., 1990).

Our original interest in the endocytic processing of β-VLDL was the strong correlation between delivery of β-VLDL to peripheral compartments and the activation of ACAT (Tabas et al., 1990, 1991). LDL is delivered rapidly to lysosomes, but it is a poor activator of ACAT, whereas β-VLDL is also delivered to peripheral compartments and strongly stimulates ACAT. In these earlier studies, we found that both the delivery to the peripheral compartment and the ability to stimulate ACAT were greater as the size of the β-VLDL increased. Furthermore, treatment with mAbs or Fabs to apoE, which reduced the effective valency of β-VLDL binding, redirected the β-VLDL so that it was delivered to lysosomes rapidly and reduced the activation of ACAT. These data are consistent with the notion that cholesterol released from lysosomes in these cells, whether derived from LDL or β-VLDL, is a rather poor stimulator of ACAT, whereas cholesterol released from peripheral compartments is a potent stimulator of ACAT. This idea would imply that although β-VLDL, once it leaves the periphery, is rapidly transported to perinuclear lysosomes (Fig. 7), it is the retention of β-VLDL for a few minutes in the periphery that is important in the ability of the lipoprotein to stimulate ACAT.

It was surprising that these peripheral compartments are actually deep tubules with open connections to the surface. Clearly, any processing of β-VLDL that takes place there is very different from the processing by acid hydrolases in lysosomes. Using fluorescence energy transfer microscopy, we were able to show that significant disintegration of β-VLDL particles does occur in the peripheral tubules. These experiments do not elucidate the molecular mechanism for processing of the lipoproteins. Macrophages do have neutral cholesterol esterases, but the localization and functional role of these enzymes are not known (Khoo et al., 1981, 1984). Other enzmyes, such as neutral sphingomyelinases (Das et al., 1984), are found externally oriented on plasma membranes, and these could act on the lipoproteins, leading to loss of integrity. Since 15% of the cholesterol in β-VLDL is unesterified (Tabas et al., 1990), disruption of the β-VLDL particle in the peripheral compartment could release free cholesterol directly to the plasma membrane. It has been shown that free cholesterol delivered to the plasma membrane can serve as an effective activator of ACAT (Tabas et al., 1988). The mechanisms for delivering cholesterol from either the plasma membrane or lysosomes to ACAT, which is thought to reside in the ER (Balasubramanian et al., 1978), are not known. Nonetheless, based on our results, we speculate that β-VLDL is an effective activator of ACAT because it is retained at the plasma membrane in deep tubules where processing occurs that releases cholesterol into a pool (i.e., the plasma membrane) that is especially effective in stimulation of ACAT. In fact, studies of HDL-mediated cholesterol removal from macrophages (Phillips and Rothblat, 1987) indicate that cholesterol can move between lipoproteins and the plasma membrane, although in our case cholesterol would be delivered to the plasma membrane by the β-VLDL. Although a mechanistic link between the surface tubules and ACAT activity is not yet established, the results

presented here demonstrate processing of β-VLDL by a novel endocytic pathway that may play an important role in the interaction of this atherogenic lipoprotein with macrophages.

We are grateful to Ms. Yueqing Li and Ms. Diane Sherman for assistance with EM autoradiography. We also wish to thank the MICROMED staff for IVEM technical assistance and EM printing.

This work was supported by National Institutes of Health (NIH) grants HL-39703 and HL-21006 (I. Tabas), HL-08372 (J. Myers), HL-41990 (N. Jones), DK-27083 (F. Maxfield), and use of IVEM facilities was funded by RR-02722. I. Tabas is an Established Investigator of the American Heart Association and Boehringer-Ingelheim, Inc.

Received for publication 9 July 1993 and in revised form 11 September 1993.

References

Bainton, D. F., R. Takemura, P. E. Stenberg, and Z. Werb. 1989. Rapid fragmentation and reorganization of Golgi membranes during frustrated phagocytosis of immobile immune complexes by macrophages. *Am. J. Pathol.* 134:15-26.

Balasubramanian, S., S. Venkatesen, K. A. Mitropoulos, and T. J. Peters. 1978. The submicrosomal localization of acyl-coenzyme A:cholesterol acyltransferase and its substrate and of cholesteryl esters in rat liver. *Biochem. J.* 174:863-872.

Brown, M. S., and J. L. Goldstein. 1983. Lipoprotein metabolism in the macrophage: implications for cholesterol deposition in atherosclerosis. *Annu. Rev. Biochem.* 52:223-261.

Brown, M. S., S. E. Dana, and J. L. Goldstein. 1975. Receptor-dependent hydrolysis of cholesteryl esters contained in plasma low density lipoprotein. *Proc. Natl. Acad. Sci. USA.* 72:2925-2929.

Dabora, S. L., and M. P. Sheetz. 1988. The microtubule-dependent formation of a tubulovesicular network with characteristics of the ER from cultured cell extracts. *Cell.* 54:27-35.

Das, D. V. M., H. W. Cook, and M. W. Spence. 1984. Evidence that neutral sphingomyelinase of cultured neuroblastoma cells is oriented externally on the plasma membrane. *Biochim. Biophys. Acta.* 777:339-342.

Dunn, K. W., and F. R. Maxfield. 1992. Delivery of ligands from sorting endosomes to late endosomes occurs by maturation of sorting endosomes. *J. Cell Biol.* 117:301-310.

Faggioto, A., R. Ross, and L. Harker. 1984. Studies of hypercholesterolemia in the nonhuman primate. I. Changes that lead to fatty streak formation. *Arteriosclerosis.* 4:323-340.

Fainaru, M., R. W. Mahley, R. L. Hamilton, and T. L. Innerarity. 1982. Structural and metabolic heterogeneity of β-very low density lipoproteins from cholesterol-fed dogs and from humans with Type III hyperlipoproteinemia. *J. Lipid Res.* 23:702-714.

Foley, M., A. N. MacGregor, J. R. Kusel, P. B. Garland, T. Downie, and I. Moore. 1986. The lateral diffusion of lipid probes in the surface membrane of *Schistosoma mansoni*. *J. Cell Biol.* 103:807-818.

Gerrity, R. G. 1981. The role of the monocyte in atherogenesis. I. Transition of blood-borne monocytes into foam cells in fatty lesions. *Am. J. Pathol.* 103:181-190.

Gershon, M. D., and D. L. Sherman. 1987. Noradrenergic Innervation of Serotoninergic Neurons in the Myenteric Plexus. *J. Comp. Neurol.* 259: 193-210.

Golan, D. E., C. S. Brown, C. M. L. Cianci, S. T. Furlong, and J. P. Caulfield. 1986. Schisotosomula of Schistosoma mansoni use lysophosphatidylcholine to lyse adherent human red blood cells and immobilize red cell membrane components. *J. Cell Biol.* 103:819-828.

Goldstein, J. L., Y. K. Ho, M. S. Brown, T. L. Innerarity, and R. W. Mahley. 1980. Cholesteryl ester accumulation in macrophages resulting from receptor-mediated uptake and degradation of hypercholesterolemic canine β-very low density lipoproteins. *J. Biol. Chem.* 255:1839-1848.

Goldstein, J. L., S. K. Basu, and M. S. Brown. 1983. Receptor-mediated endocytosis of low density lipoprotein in cultured cells. *Methods Enzymol.* 98:241-260.

Griffin, F. M., J. A. Griffin, J. E. Leider, and S. C. Silverstein. 1975. Studies on the mechanism of phagocytosis. I. Requirements for circumferential attachment of particle-bound ligands to specific receptors on the macrophage plasma membrane. *J. Exp. Med.* 142:1263-1282.

Guyton, J. R., and K. F. Klemp. 1989. The lipid rich core region of human atherosclerotic fibrous plaques: prevalence of small and vesicles. *Am. J. Pathol.* 134:705-717.

Hed, J., G. Haliden, S. G. O. Johanson, and F. Lerssen. 1987. The use of fluorescence quenching in flow cytometry to measure the attachment and ingestion phases in phagocytosis in peripheral blood without prior cell separation. *J. Immunol. Methods.* 101:119-125.

Herman, B. 1989. Resonance energy transfer microscopy. *In.* Methods in Cell Biology. D. L. Taylor and Y. L. Wang, editors. Academic Press, San Diego, CA. 30:219-243.

Hughes, E. N., and J. T. August. 1981. Characterization of plasma membrane proteins identified by monoclonal antibodies. *J. Biol. Chem.* 256:664-671.

Innerarity, T. L., R. E. Pitas, and R. W. Mahley. 1982. Modulating effects of canine high density lipoproteins on cholesteryl ester synthesis induced by β-very low density lipoproteins in macrophages. Possible *in vitro* correlates with atherosclerosis. *Arteriosclerosis.* 2:114-124.

Johnson, J. D., M.-R. Taskinen, N. Matsuoka, and R. L. Jackson. 1980. Dansyl phosphatidylethanolamine-labeled very low density lipoproteins. *J. Biol. Chem.* 255:3461-3465.

Jones, N. L., N. S. Allen, J. C. Lewis. 1991. β-VLDL uptake by pigeon monocyte-derived macrophages: correlation of binding dynamics with three-dimensional ultrastructure. *Cell Motil. Cytoskeleton.* 19:139-151.

Khoo, J. C., E. Mahoney, and D. Steinberg. 1981. Neutral cholesterol esterase activity in macrophages and its enhancement by CAMP-dependent protein kinase. *J. Biol. Chem.* 256:12659-12661.

Khoo, J. C., J. Vance, E. Mahoney, D. Jensen, E. Wancewicz, and D. Steinberg. 1984. Neutral triglyceride lipase in macrophages. *Arteriosclerosis.* 4:34-40.

Lowry, O. H., N. J. Rosenbrough, A. L. Farr, and R. J. Randall. 1951. Protein measurement with the folin phenol reagent. *J. Biol. Chem.* 193:265-275.

Maxfield, F. R. 1989. Measurement of vacuolar pH and cytoplasmic calcium in living cells using fluorescence microscopy. *Methods Enzymol.* 173: 745-771.

Maxfield, F. R., and K. Dunn. 1990. Studies of endocytosis using image intensification fluorescence microscopy and digital image analysis. *In* Optical Microscopy for Biology. Wiley-Liss, Inc. 357-371.

Maxfield, F. R., and D. Yamashiro. 1991. Acidification of organelles and the intracellular sorting of proteins during endocytosis. *In* Intracellular Trafficking of Proteins, C. J. Steer and J. A. Hanover, editors. Cambridge University Press, Cambridge. 157-182.

Mayorga, L. S., F. Bertini, P. D. Stahl. 1991. Fusion of newly formed phagosomes with endosomes in intact cells and in a cell-free system. *J. Biol. Chem.* 266:6511-6517.

Nichols, B. A. 1982. Uptake and digestion of horseradish peroxidase in rabbit alveolar macrophages. Formation of a pathway connecting lysosomes to the cell surface. *Lab. Invest.* 47:235-246.

Pastan, I., and M. Willingham. 1981. Journey to the center of the cell: role of the receptosome. *Science (Wash. DC).* 214:504-509.

Phillips, M. C., W. J. Johnson, and G. H. Rothblat. 1987. Mechanisms and consequences of cellular cholesterol exchange and transfer. *Biochim. Biophys. Acta.* 906:223-276.

Pitas, R. E., T. L. Innerarity, J. N. Weinstein, and R. W. Mahley. 1981. Acetoacetylated lipoproteins used to distinguish fibroblasts from macrophages in vitro by fluorescence microscopy. *Arteriosclerosis.* 1:177-185.

Rabinowitz, S., H. Horstmann, S. Gordon, and G. Griffiths. 1992. Immunocytochemical characterization of the endocytic and phagolysosomal compartments in mouse peritoneal macrophages. *J. Cell Biol.* 116:95-112.

Salzman, N. H., and F. R. Maxfield. 1988. Intracellular fusion of sequentially formed endocytic compartments. *J. Cell. Biol.* 106:1083-1091.

Salzman, N. H., and F. R. Maxfield. 1989. Fusion accessibility of endocytic compartments along the recycling and lysosomal endocytic pathways in intact cells. *J. Cell Biol.* 109:2097-2104.

Schaffner, T., K. Taylor, E. Bartucci, K. Fischer-Dzoga, J. Beeson, S. Glagov, and R. Wissler. 1980. Arterial foam cells with distinctive immunomorphologic and histochemical features of macrophages. *Am. J. Pathol.* 100:57-73.

Schmitz, G., H. Robenek, U. Lohmann, and G. Assmann. 1985. Interaction of high density lipoproteins with cholesteryl ester-laden macrophages. *EMBO (Eur. Mol. Biol. Organ.) J.* 4:613-622.

Schmitz, G., M. Beuck, H. Fisher, G. Nowicka, and H. Robenek. 1990. Regulation of phospholipid biosynthesis during cholesterol influx and high density lipoprotein-mediated cholesterol efflux in macrophages. *J. Lipid Res.* 31:1741-1742.

Suckling, K. E., and E. F. Strange. 1985. Role of ACAT in cellular cholesterol metabolism. *J. Lipid Res.* 26:647-671.

Swanson, J. A. 1989. Phorbol esters stimulate macropinocytosis and solute flow through macrophages. *J. Cell Sci.* 94:135-142.

Tabas, I., D. A. Weiland, and A. R. Tall. 1986. Inhibition of ACAT in J774 macrophages enhances down-regulation of the LDL receptor and HMG-CoA reductase and prevents LDL-induced cholesterol accumulation. *J. Biol. Chem.* 261:3147-3155.

Tabas, I., W. J. Rosoff, and G. C. Boykow. 1988. Acyl coenzyme A:cholesterol acyl transferase in macrophages utilizes a cellular pool of cholesterol oxidase-accessible cholesterol as substrate. *J. Biol. Chem.* 265:1266-1272.

Tabas, I., S. Lim, X. Xu, and F. R. Maxfield. 1990. Endocytosed β-VLDL and LDL are delivered to different intracellular vesicles in mouse peritoneal macrophages. *J. Cell Biol.* 111:929-940.

Tabas, I., J. N. Myers, T. L. Innerarity, X.-X. Xu, K. Arnold, J. Boyles, and F. R. Maxfield. 1991. The influence of particle size and multiple apoprotein

E-receptor interactions on the endocytic targeting of β-VLDL in mouse peritoneal macrophages. *J. Cell Biol.* 115:1547–1560.
Tycko, B., and F. R. Maxfield. 1982. Rapid acidification of endocytic vesicles containing α_2-macroglobulin. *Cell.* 28:643–651.
Uster, P. S., and R. E. Pagano. 1986. Resonance energy transfer microscopy: Observations of membrane-bound fluorescent probes in model membranes and in living cells. *J. Cell Biol.* 103:1221–1234.
Van Strijp, J. A. G., K. P. M. van Kessel, M. E. van der Tol, and J. Verhoef. 1989. Complement-mediated phagocytosis of herpes simplex virus by human granulocytes: binding or ingestion. *J. Clin. Invest.* 84:107–112.
Weersink, A. J. L., K. P. M. van Kessel, R. Torensma, J. A. G. van Strijp, and J. Verhoef. 1990. Binding of rough lipopolysaccharides (LPS) to human leukocytes. *J. Immunol.* 145:318–324.
Xu, X.-X., and I. Tabas. 1991. Lipoproteins activate acyl-coenzyme A:cholesterol acetyltransferase in macrophages only after cellular cholesterol pools are expanded to a critical level. *J. Biol. Chem.* 266:17040–17048.